ELSEVIER

Journal of Power Sources 68 (1997) 277–282

JOURNAL OF POWER SOURCES

Characterization of modified NG7 graphite as an improved anode for lithium-ion batteries

C. Menachem [a,*], E. Peled [a], L. Burstein [b], Y. Rosenberg [b]

[a] *School of Chemistry, Tel Aviv University, Tel Aviv, Israel*

[b] *The Wolfson Applied Materials Research Center, Tel Aviv University, Tel Aviv, Israel*

Accepted 17 October 1996

Abstract

Mild oxidation (burnoff) has been found to improve the performance of NG7 (natural graphite) in Li/Li_xC_6 cells. The reversible capacity of the graphite (Q_R) increased (up to 405 mAh/g for the 0–2 V range at 4–11% burnoff), its irreversible capacity (Q_{IR}) decreased with burnoff and the degradation rate of the Li_xC_6 electrode was much lower. The increase in capacity at 4–11% burnoff of NG7 was found to be associated with the formation of less than 1% void volume. On further burning beyond 11% weight loss, the density decreases faster, down to 1.92 g/cm^3 at 34% burnoff. This is associated with some decrease in Q_R. X-ray photoelectron spectrocopy studies showed that the surface oxygen content of NG7 has a broad minimum at 4–22% burnoff. The highest oxygen peak shifted monotonically with burnoff time, rising from 531.05 eV for pristine NG7 to 534.0 eV for 34% burnoff sample. The X-ray photoemission spectra may be assigned to hydroxyl surface groups in the case of the pristine sample and to surface acid groups in the case of burnt samples. From the powder X-ray diffraction and dq/dv results, it was found that a more ordered structure appears on cycling. Performance improvement was attributed to the formation of a solid electrolyte interface chemically bonded to the surface carboxylic groups at the zigzag and armchair faces, better wetting by the electrolyte and to accommodation of extra lithium at the zigzag, armchair and other edge sites and nanovoids. © 1997 Published by Elsevier Science S.A.

Keywords: Lithium-ion batteries; Oxidation; Graphite anode, Solid electrolyte interfaces

1. Introduction

Lithium-ion batteries, containing a carbonaceous anode, have excellent performance, long cycle life, fast charge and discharge rates and high energy density. In order to increase their energy density, carbons with high reversible capacity (Q_R) and low irreversible capacity (Q_{IR}), are being developed.

Q_R depends on the carbon electrode properties, temperature, current density, and type of electrolyte. Q_{IR} has been attributed to solid electrolyte interphase (SEI) formation, graphite exfoliation and other side reactions [1,2]. The development of high capacity carbons has been recently reviewed [3–6]. Explanation for the extra capacity over the theoretical value of 372 mAh/g can be found in Refs. [6,7].

We recently found [7,8] that mild oxidation (burnoff) of two synthetic graphites improves their performance in Li/Li_xC_6 cells. The reversible capacity of the graphite (Q_R) increased, its irreversible capacity (Q_{IR}) generally decreased (for less than 6% burnoff) and the degradation rate of the Li_xC_6 electrode (in three different electrolytes) was much lower than the pristine graphite. Scanning tunneling microscopy (STM) images of these modified graphites show nanochannels with openings of a few nm and up to tens of nm. It is believed that these nanochannels are formed at the zigzag and armchair faces between two adjacent crystallites and in the vicinity of defects and impurities. The improvement of the performance was attributed to the formation of SEI chemically bonded to the surface carboxylic groups at the zigzag and armchair faces, better wetting by the electrolyte and to the accommodation of extra lithium at the zigzag, armchair and other edge sites and nanovoids. Mild burnoff of highly oriented pyrolytic graphite (HOPG) samples clearly shows [9] that the oxidation rate is faster at the zigzag and armchair planes than at the basal plane. This graphite modification, following mild burnoff, was found to make the Li_xC_6 electrode performance more reproducible and less sensitive to electrolyte impurities.

Recently it was found that heat treatment at 700 °C in the presence of acetylene black improved the performance of the graphite-fiber anode [10]. Such treatment was found effec-

* Corresponding author. Tel. 972 3 6408438; fax. 972 3 6409293, e-mail: peled@post.tau.ac.il

PII S0378-7753(96)02629-8

tive for removing the surface hydroxyl and water, and for enlarging the surface area of the fiber. STM measurements [11] show circular monolayer pits in the basal plane after a 600 °C oxidation of single-crystal graphite.

The goal of this work was to characterize physically and electrochemically an oxidized Kansai Coke NG7 natural graphite as an improved anode for lithium-ion batteries.

The effect of percent burnoff, binder type and Shawinigan Black on the performance of oxidized NG7 anode will be published elsewhere [12].

2. Experimental

The electrochemical characterization of NG7 (Kansai Coke) in this work was carried out with the use of Li/Li_xC_6 cells. These 3–5 cm^2 cells consisted of a porous 40–70 μm thick graphite electrode supported by a copper foil, a lithium foil supported by a nickel Exmet screen, a Celgard 2400 separator and 1.2 M $LiAsF_6$/EC:DEC (1:2) electrolyte. The graphite electrodes were made by the doctor-blade technique, spreading paste which consisted of 5% Teflon (in emulsion), 5% Shawinigan Black (SB) carbon and 90% NG7 powder. NG7 powder was oxidized (partially burnt) in air at 550 °C inside a common laboratory oven (for 2.6, 4.3, 11, 22, and 34% burnoff). Cell-cycling tests were carried out on a 16 Bit Maccor 2000 Battery Tester mostly over the 0.8–0.01 V range. More experimental details can be found in Ref. [7].

Powder X-ray diffraction (PXRD) tests were carried out with the use of a Scintag θ:θ powder diffractometer with Cu Kα radiation. The electronic structure of pristine and burnt samples was analyzed by X-ray photoelectron spectroscopy (XPS). XPS measurements were carried out using a 5600 multi-technique system (Physical Electronics, USA) with a monochromatic Al Kα source (1486.6 eV). The spectra were obtained at a high resolution mode at a pass energy of 11.75 eV with 0.05 eV/step intervals. The binding energies were measured with an accuracy of ± 0.1 eV and referenced to the Au 4*f* peak at 84 ± 0.1 eV. No charging was observed on the investigated surfaces. Curve fitting was based on the modified Gauss–Newton non-linear least-squares optimization procedure.

Scanning electron microscopy (SEM) images were taken with the use of a JEOL, JSM-3600 microscope.

3. Results and discussion

SEM micrographs (Fig. 1) show that on burning, the smallest and largest NG7 particles disappear leaving only medium-size particles. This may result from preferential burning of less-ordered zones such as small particles and zones containing defects or impurities. Electrostatic charging of oxidized graphite samples is less of a problem, and higher resolution can be achieved compared with the pristine graphite. This indicates that oxidation enhances the electronic conductivity of the graphite, probably making it a p-type semiconductor. The adsorption of benzene (from the vapor phase on the synthetic graphite) at 20 °C dropped by about 30% after 28% burnoff [13], indicating a decrease in surface area of the sample. Pycnometric measurements, with the use of diethyl carbonate (DEC) as the pycnometer liquid, reveal (Fig. 2) two slopes in the density–% burnoff curve. The density of pristine NG7 is 2.19 g/cm^3. There is very little change in density (less than 1%) from 0–11% burnoff and it drops sharply to 1.92 g/cm^3 at 34% burnoff. This indicates the formation of closed pores, not accessible to the DEC molecule, with a void volume of less than 1% at 11% burnoff and 12.7% at 34% burnoff. DEC was chosen for this test because it is the major component of the electrolyte in lith-

Fig 1. SEM graphs of: (a) pristine sample, and (b) 34% burnoff sample.

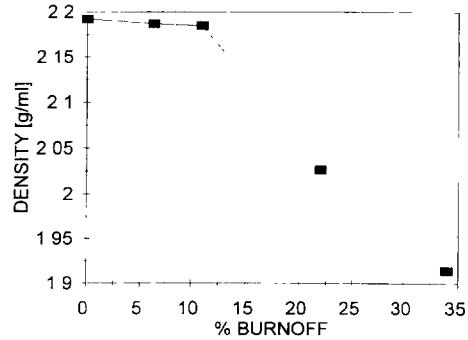

Fig. 2. Effect of burnoff on density.

ium-ion batteries and in our tests. Some of this void volume may accommodate extra lithium. Changes in surface groups on NG7 were determined with the use of XPS. The surface oxygen content changes with the amount of burnoff (Fig. 3). It is 8% atomic concentration in the pristine NG7, drops to 2.5% at 4.3% burnoff, stay about constant up to 22% burnoff and rises again to 17% in the 34% burnoff sample. The decrease in oxygen content may be correlated with the preferential burnoff of small particles and disordered area, as the oxygen is chemically bonded only to edge sites (such as zigzag and armchair planes) and not to the basal plane. It is in agreement with the rise in the basal to zigzag and armchair area ratio found for oxidized HOPG samples [9]. The rise in oxygen content with further burning may be associated with atomic scale roughness, not seen by SEM. Fig. 4 compares the C(1s) peak of the pristine with that of 11% and 34% burnoff samples. The O(1s) peaks of the same surfaces are presented in Fig. 5. The shape of the 34% burnoff carbon peak at the high energy side demonstrates the presence of highly oxidized components in a double-bond-oxygen and acid configurations. At low percentage of burnoff, the oxygen peak better represents the chemical changes than the carbon peak. For 11% burnoff the oxygen peak maximum is shifted from the pristine (531 eV) to higher energies (533.35 eV), as in the case of the 34% burnoff, when the peak maximum is observed at an energy of 533.75 eV. This tendency of oxygen peaks shift to higher energies can be the evidence of the acid-bonding character [14] induced by the mild oxidation process.

The same conclusions, concerning the appearance of the acid groups with burning, can be drawn from comparison of the C(1s) peaks for the pristine and 34% burnt sample after curve fitting procedure (Figs. 6 and 7, respectively). Fitting parameters and peak assignments are presented in Table 1. Peak shifts are referred to peak No. 3, the main peak, which is assigned to aromatic carbons not bonded to oxygen or hydrogen (C–C bond). This peak is found to be at 284.1 eV

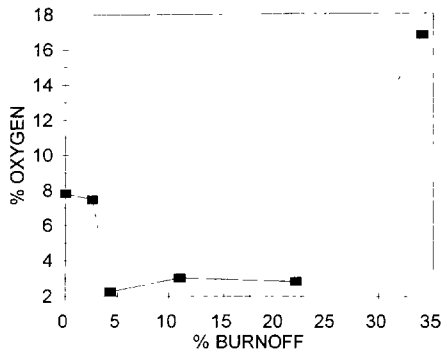

Fig. 3. XPS measurements: effect of burnoff on surface oxygen content

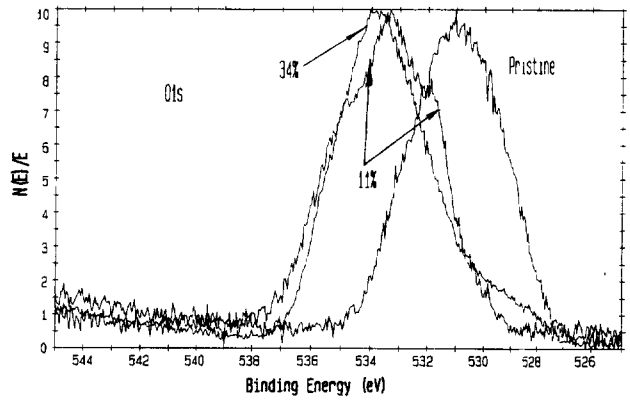

Fig. 5 XPS measurements: effect of burnoff on the O(1s) spectra (normalized spectra)

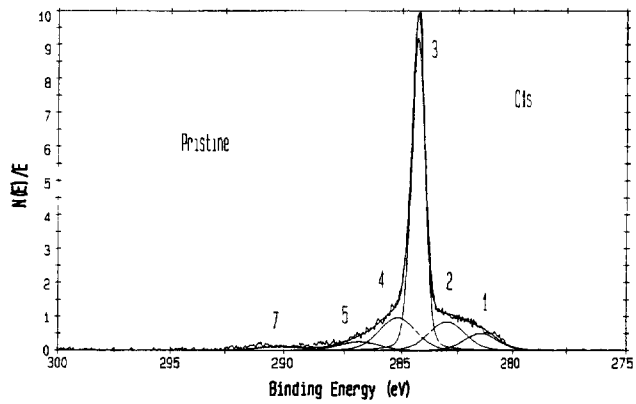

Fig. 6. XPS measurements: fitting results for the C(1s) spectra, pristine sample

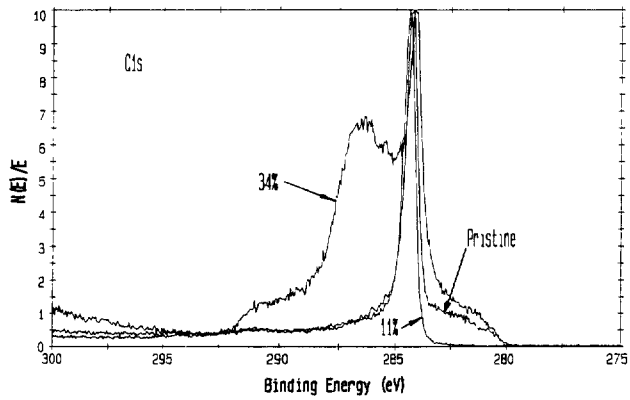

Fig 4. XPS measurements: effect of burnoff on the C(1s) spectra (normalized spectra).

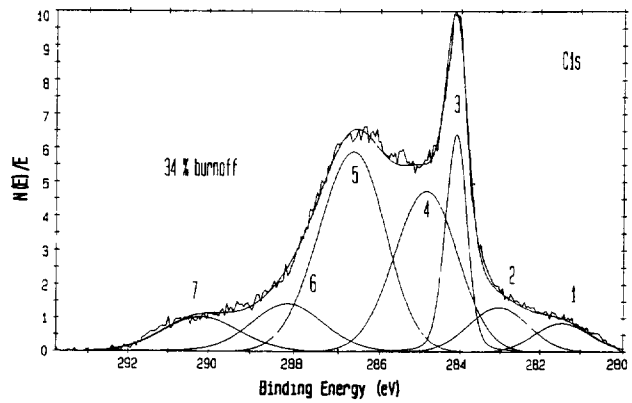

Fig 7. XPS measurements: fitting results for the C(1s) spectra, 34% burnoff sample

Table 1
Binding energies and fitting parameters of the C(1s) curves for the pristine and 34% burnt samples

Peak No	Sample	Peak position (eV)	Peak shift (eV)	FWHM (eV)	% of total area	Peak assignment
1	Pristine	281.48	2.8	1.5	5.2	Hydrocarbons
	34%	281.5	2.6	1.6	4.1	
2	Pristine	283.0	1.3	2.1	15.4	Hydrocarbons
	34%	283.0	1.1	1.8	7	
3	Pristine	284.3	0	0 68	53	Aromatic carbon, C–C
	34%	284.1	0	0 63	13.4	
4	Pristine	285.2	0.9	2.1	19 5	C–OH
	34%	284.9	0 8	1 9	26.6	
5	Pristine	286.9	2.6	2.1	4.8	C=O
	34%	286.7	2.6	1.9	33.1	
6	Pristine					
	34%	288.2	4.1	1.9	8 9	O=C–OH
7	Pristine	290.2	5 9	2.2	2 1	Shake-up satellite
	34%	290.1	6 0	2.2	6.8	

Table 2
Experimental intensity ratios of different oxygen groups relative to carbon–carbon bonding

Sample	C–C/C–OH (I_3:I_4)	C–C/C=O (I_3:I_5)	C–C/O=C–OH (I_3:I_6)
Pristine	1:0.4	1:0.9	1:0
34%	1 2	1:2 5	1:0.7

in the case of 34% burnoff and at 284.3 eV for the pristine which is typical for graphite [15,16]. It is obvious from comparison of Figs. 6 and 7 that peak No. 6 is present on the 34% burnt surface only. This peak is shifted by 4.1 eV from the C–C peak and can be attributed to the carboxylic group connected to the aromatic carbon (O=C–OH) [17]. This result suggests that surface acid groups are important products of the mild oxidation process.

The shoulder at the low energy side of the main carbon peak, approximated by two peaks (Nos. 1 and 2, Figs. 6 and 7), can be caused by C–H bonds [18]. The shifts of these peaks from the main peak for the pristine and burnt surface are not identical, which may point to the different C–H groups formed by oxidation. Peak No. 7 is shifted by 6 ± 0.1 eV from the C–C peak for both samples. This shift is due to the $\pi^* \leftarrow \pi$ shake-up satellite [19].

Peak No. 4 is revealed in both cases with a shift of 0.9 eV. It is characteristic of an aromatic carbon singly bonded to oxygen [20] and can be assigned to hydroxyl groups (C–OH).

Peak No. 5 is observed on the pristine and the 34% burnt sample with the same shift of 2.6 eV. This shift is typical of the C=O groups [15]. Although C–OH and C=O groups are present on both the pristine and mildly oxidized surfaces, their intensity (area under the peak) increases with oxidation as compared with the C–C groups (Table 1). Acid groups are induced by mild oxidation as an integral feature of this process. This is summarized in Table 2, which gives the ratios of the peak areas for peaks Nos. 4–6 (I_4, I_5 and I_6) to that of No. 3 (I_3).

In summary, oxidation of NG-7 results in a decrease in the content of C–H groups (Table 1), in an increase in the content of aromatic C–OH and C=O groups and in the formation of acid (COOH) groups (which are absent in the pristine sample).

Table 3 summarizes the effect of oxidation on Q_{IR}, Q_R and the degradation rate. The reversible capacity of NG7 meas-

Table 3
Effect of burnoff on performance

% burnoff	x in Li_xC_6 [a]	Q_t (mAh/g)	Irreversible capacity (mAh/g)		Degradation rate (%/cycle)	
			Q_{IR} [b]	Q_{IR1} [c]	50 μA/cm²	C/4
P	0.94	350	159	199	1.5	1.3
2 6	0.89	331	151	190	1.5	
4.3	1.05	391	138 [d]	170	0 5	0.8
11	1.05	391	141	174	0.3	0.6
34	0 92	342	126	164	1 8	0.9

[a] for 0 8–0 01 V range, 50 μA/cm²
[b] Q_{IR}, irreversible capacity in the first cycle.
[c] Q_{IRT}, irreversible capacity in the first five cycles.
[d] first intercalation at C/4, 4 h at 10 mV

ured over the 0.8–0.01 V range increases from 350 mAh/g for the pristine sample to 390 mAh/g for 4.3% and 11% burnoff samples and decreases to 340 mAh/g for 34% burnoff sample. Increasing the cycling voltage range from 0.8–0.01 to 2.0–0.00 V resulted in an increase of about 4% to the reversible capacity. Taking into account this correction the capacity of 4–11% burnoff samples would be 405 mAh/g or $x = 1.1$ in Li_xC_6. The irreversible capacity, measured in the first cycle, drops monotonically with burnoff time from 159 mAh/g for the pristine NG7 to 126 mAh/g for a 34% burnoff sample. It was further decreased to 92 mAh/g for a SB-free pristine sample. The lowest Q_{IR} was measured at high current density first charge and was 54 mAh/g for the 11% burnoff sample free of SB [12]. It is interesting to note that the increase in Q_R for 4.3% and 11% burnoff samples is associated with the formation of only 1% void volume (Fig. 2) and further increase in void volume (by oxidation) results in a decrease in Q_R (Table 3). This may indicate that only very small voids (on an atomic scale) can accommodate the extra reversible lithium capacity. The fact that on further burning, graphite density decreases to 1.9 g/cm^3 while no more lithium is inserted, can be explained by lithium accommodation which is one or at most a few layers, on the inner walls of these voids, with no bulk lithium aggregate being formed.

The decrease in Q_{IR} with partial oxidation is in agreement with the SEM observation and adsorption tests indicating a decrease in surface area of the modified NG7. The Faradaic efficiency in the first few (five) cycles is lower than 100%. It is somewhat higher for the modified NG7 samples than for pristine samples [12]. The degradation rate at 50 μA/cm^2 is an average for the first five cycles, and the value for the $C/4$ rate is an average of the consecutive 50 cycles (Table 3). The slowest degradation rate was measured for 11% burnt sample. SB-free electrodes were found to degrade five times faster than electrodes containing 5% SB. There are some indications that particle disconnection is responsible at least for part of the anode degradation.

The (002) and (004) NG7 powder XRD peaks became narrower on cycling (Table 4) as was previously found for synthetic graphite [21,22]. This indicates an increase in L_c (i.e. more ordered structure of the graphite). This is in agreement with dq/dv results (Fig. 8 and Ref. [22]) where reversibility is improved during the cycling process. After two days of rest after cycling the width of both (002) and (004) peaks rose close to their original values (Table 4), indicating an decrease in L_c value.

Table 4
Effect of cycling of 11% burnoff sample on the FWHM (full-width at half maximum) of the 002 and 004 Bragg peaks

	(004) Peak (°)	(002) Peak (°)
Before cycling	0.129	0.162
After cycling	0.099	0.131
Two days after cycling	0.123	0.143

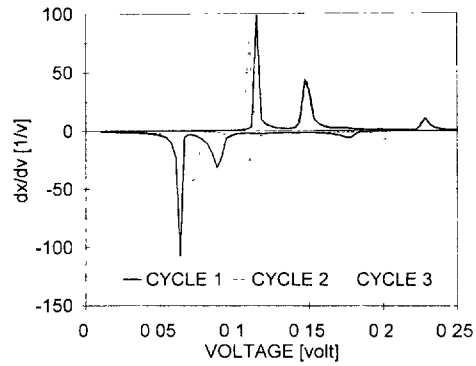

Fig. 8. Effect of cycling on dq/dv plot, 11% burnoff sample.

4. Conclusions

The improvement of the performance is attributed to the formation of SEI chemically bonded to the surface carboxylic groups at the zigzag and armchair faces, to the decrease in surface area and to the accommodation of extra lithium at the zigzag, armchair and other edge sites and atomic scale voids.

Acknowledgements

The authors would like to thank Kansai Coke for supplying NG7 powder.

References

[1] R. Fang, U Von Sacken and J.R. Dahn, *J. Electrochem Soc., 137* (1990) 2009
[2] R Kanno, Y. Kawamoto, Y. Takeda, S. Ohashi, N Imanishi and Y Yamamoto, *J Electrochem. Soc., 139* (1992) 3397.
[3] J.R Dahn, A K Sleigh, H. Shi, J.N Reimers, Q. Zhong and B.M. Way, *Electrochim. Acta, 38* (1993) 1179.
[4] J.R. Dahn, A.K. Sleigh, H Shi, B.M. Way, Y J. Weydanz, J.N. Reimers, Q. Zhong and U Von Sacken, in G. Pistoia (ed.), *Lithium Batteries, New Materials and New Perspectives*, Elsevier, Amsterdam, 1993.
[5] R Yazami, in G. Pistoia (ed.), *Lithium Batteries, New Materials and New Perspectives*, Elsevier, Amsterdam, 1993.
[6] J.R. Dahn, T Zheng, Y Liu and J.S. Xu, *Science, 270* (1995) 590.
[7] E Peled, C Menachem, D. Bar-Tow and A Melman, *J Electrochem. Soc., 143* (1996) L4.
[8] E. Peled, D. Golodnitsky, G. Ardel, C. Menachem, D. Bar-Tow and V. Eshkenazy, in D H Doughty et al (eds.), *Proc. 1995 MRS Meet., San Francisco, CA, USA*, Proc. Vol 393, 1995. p. 209
[9] D. Bar-Tow and E Peled, unpublished results.
[10] T Takamura, M. Kikuchi and Y. Ikezawa, in S Megahed, B.M. Barnett and L Xie (eds.), *Rechargeable Lithium and Lithium-ion Batteries*, The Electrochemical Society Proc. Series, PV 94-28, Pennington, NJ, USA, 1995, p. 213.
[11] X Chu, W.H. Smyrl and L.D. Schmidt, in S. Megahed, B M. Barnett and L. Xie (eds.), *Rechargeable Lithium and Lithium-ion Batteries*, The Electrochemical Society Proc. Series, PV 94-28, Pennington, NJ, USA, 1995, p. 196.
[12] C. Menachem, E. Peled and L. Burnstein, *37th Power Sources Conf., NJ, USA, June 1996*, p 208.

[13] C. Menachem and E. Peled, unpublished results.

[14] D Briggs and M.P Seah, *Practical Surface Analysis, Vol. 1, Auger and X-ray Photoelectron Spectroscopy*, Wiley, New York, 2nd edn., 1990, p. 470.

[15] S. Basu, G.K. Wertheim and S.B. Dicenzo, in R.O. Bach (eds.), *Lithium: Current Application in Science, Medicine and Technology*, Wiley-Interscience, New York, 1985, p. 187.

[16] U. Gelius, P.F. Heden, J. Hedman, B.J. Lindberg, R. Manne, R. Nordberg, C. Nordling and K. Siegbahn, *Phys. Scr., 2* (1970) 70

[17] D T Clark and H.R Thomas, *J. Polym. Sci., Polym. Chem. Ed., 16* (1978) 791.

[18] D.P. Dowling, M J Ahern, T.C. Kelly, B.J. Meenan, N.M.D Brown, G.M. OíConnor and T.J. Glynn, *Surf Coat Technol., 53* (1992) 177.

[19] D T. Clark and A. Dilks, *J. Polym. Sci., Polym. Chem. Ed., 14*, 533 (1976)

[20] L.P. Buchwalter, B D. Silverman, L Witt and A.R. Rossi, *J. Vac. Sci. Technol., A5* (1987) 226.

[21] E. Peled, D. Bar-Tow, A. Melman, E. Gerenrot, Y. Lavi and Y Rosenberg, *Proc. The Electrochemical Society Fall Meet., New Orleans, LA, Oct. 1993*, Proc. Vol. 94-4, p. 177.

[22] E. Peled, in S. Megahed, B.M Barnett and L. Xie (eds.), *Rechargeable Lithium and Lithium-ion Batteries*, Proc. Vol 94-28. The Electrochemical Society, Pennington, NJ, USA, 1995, p 1